Compensation of Simultaneous Orientation Contrast in Superimposed Textures

Rudolf Netzel, Nils Rodrigues, Anja Haug and Daniel Weiskopf
Visualization Research Center (VISUS), University of Stuttgart, Germany

Keywords: Simultaneous Contrast, Texture Orientation, Human Vision.

Abstract: We propose a method that compensates the simultaneous orientation contrast in the visualization of superimposed textures. Such superposition plays a role in visualizations that overlay or enrich visual representations of data with additional information. Our compensation method extracts the direction and frequency within the input textures by using a Gabor filter bank. The foreground texture is then rotated to counterbalance the tilt illusion. The rotation angle is determined by a model that adopts results of previous studies that measured the influence of perceived contrast, direction, and frequency on the perceived tilt. The effectiveness of our method is demonstrated for artificial stimuli and a typical example of scientific flow visualization of multiple vector fields.

1 INTRODUCTION

Visualization is used to generate graphical representations of data that are more understandable than the source data in its original form. A multitude of different methods have been developed for a variety of application domains, for instance, in flow visualization to make the structure of vector fields visible, or in network visualization to show relationships between elements represented as node-link diagrams. Such visualizations often suffer from visual clutter that could, if not addressed properly, influence the perception and thereby the interpretation of visualized data. This is especially true when a post-processing step adds further information to an existing visualization by superimposition.

A specific example of such a visualization is the display of a first vector field through line integral convolution (LIC) and the overlay of arrow glyphs for a second vector field. Other examples of such overlays are points of interest and routing instructions on top of topological maps that help users to keep contextual awareness. In general, this concept is related to the topic of superimposing textures. In some cases, the method of overlaying textures may produce perceptually inconsistent results. It is even possible that optical illusions are created that falsify the visualization. In such scenarios, rendered graphics accurately depict the source data, but human perception introduces additional artifacts or distortions in addition to existing graphical features.

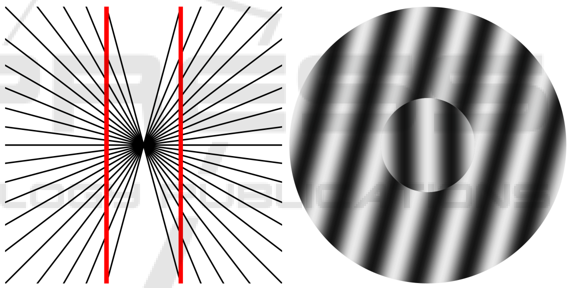

(a) Hering illusion (b) Tilt illusion

Figure 1: Examples of visual illusions. In the Hering illusion (a), two straight foreground lines (red) drawn on radial lines in the background seem to bend outwards. The tilt illusion (b) arises from a perfectly vertical texture (small inner disk) on a background. Both shapes have a sinusoid texture, but the foreground seems to have rotated counterclockwise.

One illusion that is very likely to appear in many line-based visualizations is the tilt illusion. It results in the perception of rotated or bent lines instead of straight ones (Figure 1). It is difficult to quantify the effect for a general public, as it depends on viewing distance, frequencies in the stimulus, orientation between back- and foreground, as well as individual human learning.

With this paper, we want to increase awareness of such effects within the visualization community. It is a relevant topic because it can occur when overlaying textures or even in such simple cases where lines cross

Netzel, R., Rodrigues, N., Haug, A. and Weiskopf, D.
Compensation of Simultaneous Orientation Contrast in Superimposed Textures.
DOI: 10.5220/0007356800480057
In *Proceedings of the 14th International Joint Conference on Computer Vision, Imaging and Computer Graphics Theory and Applications (VISIGRAPP 2019)*, pages 48-57
ISBN: 978-989-758-354-4

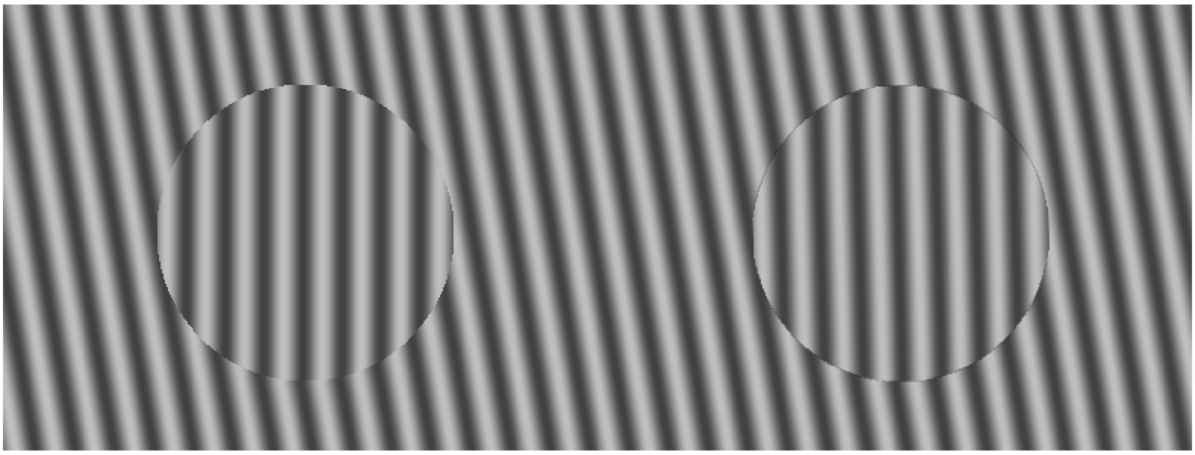

(a) Image without compensation (b) Image with compensation

Figure 2: Example of a location-dependent compensation of the simultaneous orientation contrast (tilt illusion). The images illustrate a disk (foreground texture) that is superimposed over a background texture. Both the background texture and disk exhibit sinusoidal patterns. After the compensation, the disk in (a) appears no longer rotated in (b).

(Figure 1a). This is especially problematic when the direction has to be estimated correctly, e.g., graph visualizations that use partial links (Becker et al., 1995).

For the remainder of this paper, we focus on illusions caused by the simultaneous orientation contrast. We propose a method that allows us to compensate the tilt illusion in specific cases: it takes as input two superimposed textures and determines perceived directions and frequencies of these textures utilizing Gabor filters. Our method then compensates the tilt illusion by rotating the overlaid texture in the opposite orientation (Figure 2). We show examples of orientation contrast compensation for artificial stimuli and an application from scientific visualization that we mentioned earlier: flow visualization of two superimposed vector fields, one shown by LIC, the other one shown by arrow glyphs overlaid on top of the LIC image (see Figure 7). Our model is capable of performing a compensation for such stimuli, since it operates on position-dependent data. Therefore, it can be applied for, e.g., scientific visualizations with superimposed textures.

2 RELATED WORK

When it comes to creating visualizations, there are many factors that need to be considered, e.g., which graphical primitives or color encoding should be used. The visualization research community is very well aware of the importance of human visual perception in this context (Ware, 2012). In particular, there is previous work on the role of attention (Healey and Enns, 2012; Frintrop et al., 2010) and color (Zhou and Hansen, 2016) for visualization.

However, there is less prior work that would quantify the—possibly subtle—effects of the surrounding on the actual visualization. A typical example is the simultaneous contrast effect. Quite often this effect is considered for color or luminance contrasts. For example, the simultaneous color contrast has been considered in visualization techniques. This effect causes the same color to be perceived differently depending on its surrounding colors. Mittelstädt et al. (2014) developed an algorithm for the compensation of the simultaneous color contrast by optimization of perceived color. Here, the colors of a background and a foreground texture are adjusted in an iterative process. In each iteration, the background texture is evaluated based on a color appearance model (iCAM) and adjusted accordingly. In subsequent work, Mittelstädt and Keim (2015) extended the approach to account for interpersonal differences.

Another example is the compensation of perceived motion in animated visualizations by Weiskopf (2004). Differences in perceived speed are caused by suboptimal motion perception for (almost) isoluminant colors; and these differences are compensated by data acquired through time-consuming user calibration. However, we are not aware of any previous visualization work that would compensate the perceived direction of textures, which is the focus of our paper.

Researchers have studied the tilt illusion outside the visualization context. Goodenough et al. (1979) tackled it from the psychophysical side and tried to find the causes for errors in rod and frame tests. They found that eye torsion and illusionary self-tilt do not account for the total strength of the tilt-effect. Instead, they suggested that simultaneous orientation contrast is involved in the creation of errors in rod and frame tests. Westheimer (1990) analyzed the effects of distance, surrounding lines, time duration, and synchronicity on orientation contrast for lines.

Research by Nothdurft (1991) shows that even without overlaying images, orientation contrast can create the perception of segmentation in fields of lines. This might also be relevant for visualizations where fields of arrows are superimposed on LIC images, as in our example in Section 5. Depending on the difference on the perceived main direction of a background and a foreground texture, the texture on top could appear rotated and introduce areas of inconsistent flow directions. Schwartz et al. (2009) detected the patterns of tilt illusions in natural images with spatially limited search fields and measured the perceived tilt, but they did not perform any compensation. In other research, it was shown that the spatial frequency as well as the contrast has an influence of the perceived tilt bias. To this end, Georgeson (1973) reported the tilt bias for different spatial frequencies of foreground and background texture. Durant and Clifford (2006) studied the tilt effect by presenting foreground and background asynchronously, while also varying the contrast of both. Wei et al. (2013) modeled simple cells as Gabor patches and used them to identify line segments that seem to deform when lines are crossing, but no compensation was performed. Franceschiello et al. (2018) also used this model for simple cells to derive a model that specifically compensates Hering illusions.

In general, illusions, like the tilt illusion or illusionary contours, are caused in the first two layers (V1 and V2) in the visual cortex (Molotchnikoff and Rouat, 2012; Carter, 2014). It was shown that the receptive fields of so-called *simple cells* are involved, which detect edges by overlapping receptive fields and lateral inhibition. For our paper, we adopt previous work and experiments in texture perception and make them usable for visualization by deriving a computational model for orientation compensation of superimposed textures.

The superposition of visual elements, such as textures, plays an important role in visualization whenever there is more information to be shown than just on a single 2D plot. A typical example is the combination of two surface displays (Bair and House, 2007; Bair et al., 2009) or weaving of visual regions (Luboschik et al., 2010). We are particularly interested in the simultaneous display of multivariate or multiple 2D flows in a single image (Kirby et al., 1999; Urness et al., 2006). For this, the overlay of two textures is a useful and common approach since textures can show flow direction effectively. However, none of the above previous papers considered simultaneous contrast effects in orientation perception.

3 METHOD

In this section, the compensation process for the simultaneous orientation contrast is described in more detail. Our method relies on two textures as input: one texture is a designated background texture, while the other one is the foreground texture that is being superimposed in order to provide, e.g., additional information at designated locations. The locations of foreground textures are also an input for our method.

As depicted in Figure 3, the compensation process consists of three parts: (1) *input texture analysis* to retrieve characteristic values from the textures, (2) computation of the *tilt angle model* that estimates perceived orientation, and (3) the actual compensation of the tilt bias by means of *foreground rotation*.

3.1 Input Texture Analysis

First, input textures have to be analyzed to perform the compensation. Here, perceptually relevant characteristic values are retrieved from the input textures: direction, spatial frequency, and contrast. The contrast of the textures is defined as the difference between the brightest and darkest texture point. We use Gabor filters to retrieve frequency and direction information from the textures. These kinds of filters are commonly used to imitate the frequency and direction perception in the human visual system (Palmer, 1999). Neurons and their associated receptive fields in combination with lateral inhibition of neighboring neurons form a pattern that is similar to that of Gabor filters, which are generated by multiplying a 2D sinusoidal function with a 2D Gaussian function or a Hamming window. These filters are sensitive to the direction and frequency defined by a sinusoidal function.

Our computational model performs a convolution of the input texture with these Gabor filters. The filtering result highlights edges that have properties similar to those of the sinusoidal functions of the filters. For our implementation, we create a filter bank for directions between 0° and 179°, while the frequencies are set to 2^i cycles per degree with $i \in 0,...,5$ (assuming a screen resolution of 1920×1200 and a viewing distance of 60 cm). This results in 1080 2D filter responses. A sampling of the direction in 1° steps was performed to ensure that possible maxima are not overlooked. Furthermore, the used tilt bias function

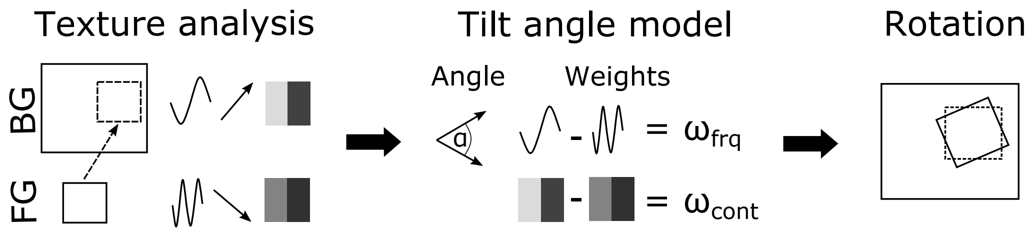

Figure 3: Steps for the compensation of the simultaneous orientation contrast. First, characteristic values are retrieved from the foreground (FG) and background (BG) textures: direction, spatial frequency, and contrast. Then, the adjusted tilt bias angle is determined; the original tilt bias angle is modified by taking into a count weights for the frequency and contrast. In the final step, the foreground object is rotated based into the opposite direction of the adjusted tilt bias.

was also derived with the same sampling. We aggregate the scalar values of each such response to get a single number that represents the total strength of each filter. We used the default parameter for the spatial frequency bandwidth (1 octave) that determines the cutoff of the filter response as frequency content in the input image doubles compared to the preferred frequency. The default parameter is also used for the spatial aspect ratio (0.5), which controls the ellipticity of the Gaussian envelope. To make these representative scalar values comparable, they are normalized by the size of their corresponding filter. The minimum size of the filters was 53×53 pixels and the maximum size 209×209 pixels. Furthermore, to compute the dominant direction and frequency, we need to aggregate the previous results in two ways: we combine all filter responses for each direction and all values for each frequency. Figure 5 shows the result of such a filter process for the first case. We determine primary directions and frequencies based on the maxima of the normalized responses.

It is important to note that Gabor filtering leads to a spatially dependent computation of the characteristic values for the texture, i.e., angle, spatial frequency, and contrast are not necessarily constant for the texture but may vary from location to location. While many of the stimuli used in perception research may have constant characteristic values across the whole image, realistic examples from scientific visualization will usually be spatially dependent.

3.2 Tilt Angle Model

In the second part, these characteristic values are used to estimate the perceived angle tilt at the respective location, i.e., the characteristic values are accessed at the position where the foreground and background textures coincide.

To this end, we adopt findings from previous studies and models from vision research and cast them into a computable model. We determine an adjusted tilt bias angle $\tilde{\alpha}_{bias}$ by multiplying the original tilt bias angle α_{bias} with weights for the influence of the spatial frequency ω_{frq} and the contrast ω_{cont}:

$$\tilde{\alpha}_{bias} = \alpha_{bias} \cdot \omega_{frq} \cdot \omega_{cont} \quad (1)$$

The values of α_{bias}, ω_{frq}, and ω_{cont} are computed by utilizing three functions that are based on previously conducted studies about the effects of the tilt bias with respect to differences of directions, frequencies, and contrasts. The first function approximates the original tilt bias angle. The directional bias is defined on the interval $[0;180]$ and is based on experimental results of Schwartz et al. (2009).

We defined the other two functions piecewise and use them as weights for the influence of spatial frequency (Georgeson, 1973) and contrast (Durant and Clifford, 2006). Figure 4b shows how the influence of frequency is defined on $[-3;0]$ and $[0;2]$ separately. Weights for contrast are available for the input ranges $[-100;0]$ and $[0;100]$ (Figure 4c). They indicate that the difference of frequency or contrast of the foreground and background texture influence the effect of tilt bias.

The influence of spatial frequency differences between foreground and background textures has an exponential drop-off in both positive and negative directions. For contrast differences, on the other hand, the dependency of the weight function is approximately linear for positive and negative values. Note that only Georgeson (1973) conducted an experiment to explicitly measure the effect of spatial frequency, while Durant and Clifford (2006) were interested in the after effects of tilt illusions (delayed presentation of background or foreground texture). This included also the simultaneous presentation of both textures, resulting in four measurements that were used to approximate the contrast weight function. Effects of tilt bias under different conditions for artificial stimuli are depicted in Figure 6 (images in the top row).

3.3 Foreground Rotation

In the last part, $\tilde{\alpha}_{bias}$ is finally used to compensate for the tilt bias. We rotate the foreground texture around

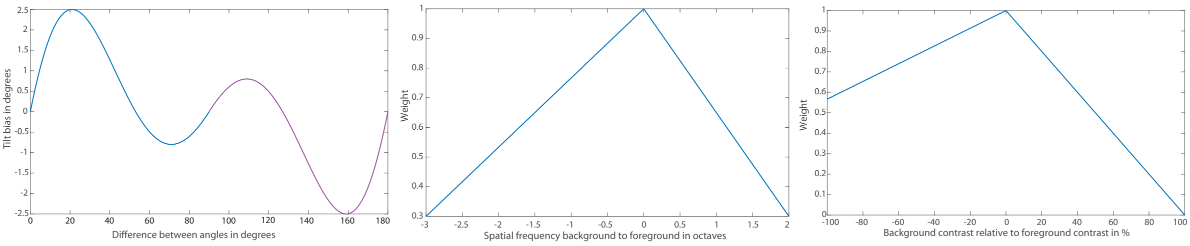

(a) Directional bias (b) Frequency weight function (c) Contrast weight function

Figure 4: Bias functions used in our tilt angle model: (a) Approximated function of the measured tilt bias of Schwartz et al. (2009); the blue part corresponds to positive angular differences in their work, magenta to negative differences. (b) Weights for the detected spatial frequency of the foreground and the background texture; the weight is one if spatial frequency has an influence, and zero if not; based on Georgeson (1973). (c) Weight for the contrast difference between the foreground and background texture; the weight is one if the contrast has an influence, and zero if not; based on Durant and Clifford (2006).

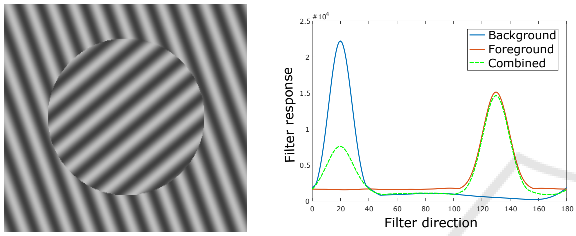

(a) Superimposed images (b) Responses of filters

Figure 5: Result of applying a Gabor filter bank on a superimposed image (a). The plot (b) shows the responses of the filters in tested direction for the foreground, background, and superimposed image. Maxima indicate the main directions.

its center point by the opposite of the adjusted tilt bias angle.

This approach works quite well as long as the foreground object covers a rather small area so that the spatial coincidence between foreground and background can be uniquely determined. Furthermore, a small object may just be rotated as a whole without further considerations to be made. We leave the extension of our method to large foreground objects for future work: it may have to include nonlinear deformations of the foreground texture to accommodate spatially varying tilt angles.

4 ARTIFICIAL STIMULI

During the development and refinement of our compensation method, we used a series of test images to qualitatively rate the compensation. One series of test images contained alternating black and white bars, where both foreground and background texture had a rectangular shape. Corners and edges of the foreground textures might be useful for the visual system to perform some kind of implicit compensation. Hence, we used circular foreground textures in other tests. Additionally, we employed sinusoidal functions to generate striped textures. Related work often uses such kinds of stimuli in the context of measuring the tilt bias.

We went through several trial-and-error cycles to detect and address problems with our preliminary compensation model. The filter responses are one example. At first, they were noisy and it was not possible to detect a maximum, since the sizes of filters were not considered. Therefore, we introduced a normalization of filter responses.

Initial tests with textures of the same contrast and spatial frequency yielded good results. However, the method produced an overcompensation when we changed the spatial frequency between foreground and background. As described in the previous section, weighting the compensation by the differences in spatial frequency addressed this issue. For the same reasons, a weight for the contrast difference was introduced. We were able to prevent overcompensation with these countermeasures. Results of successful compensations for simple cases are depicted in Figure 6 (images on the bottom).

The test stimuli used so far are based on frequencies and local contrasts that are constant across the image. To further demonstrate the effects of tilt bias and the results of our compensation method, we created images that contain a broad range of frequency, direction, and local contrast changes by using a Jähne test pattern (Jähne, 2004). In such images, the spatial frequency increases continuously from the center until reaching a defined maximum at the outer border. That makes the patterns point-symmetric and allows for tests with a continuous range of directions. So far, the stimuli have always been monochrome. We continue without introducing color and calculate the brightness of each point in the image using the

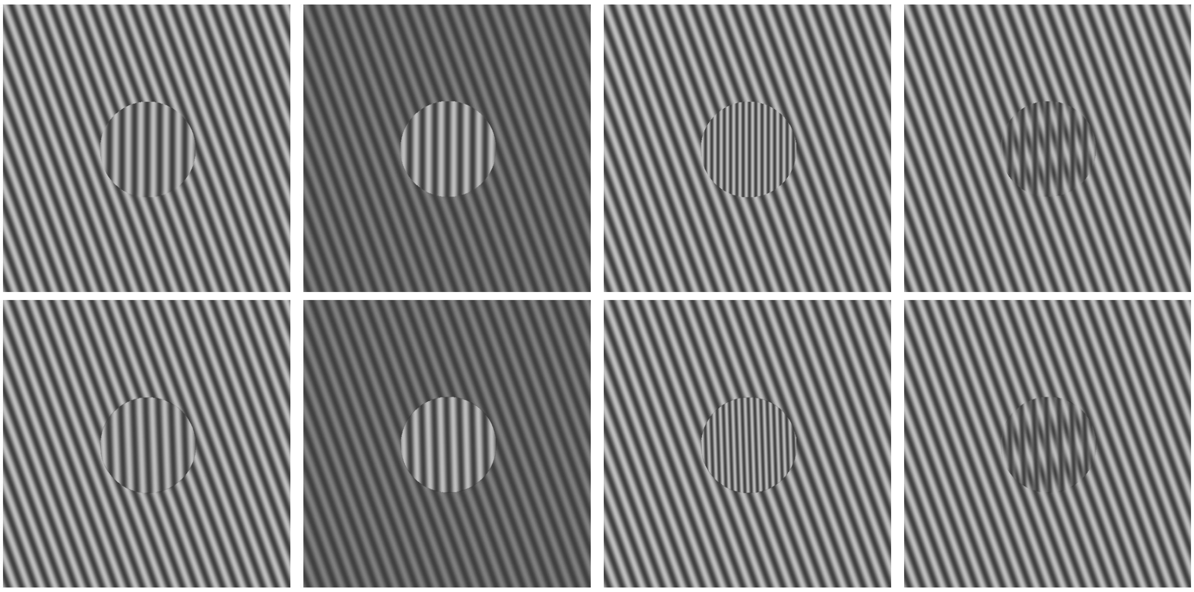

(a) No differences (b) Contrast difference (c) Frequency difference (d) Transparency

Figure 6: The tilt bias is influenced by the spatial frequency and contrast difference of the foreground and the background texture. The effect is also present if transparency is used. This is shown in the top row. The bottom row depicts the same images under the same conditions and after the compensation. In the bottom images of (a) and (d), the compensation was not affected by the contrast and frequency weight. In (b) and (c), the weights reduced the amount of compensation. Viewing distance about 20 cm.

function

$$g(x) = g_0 \cdot \sin\left(\frac{k_m|x|^2}{2r_m}\right) \cdot \left[\frac{1}{2}\tanh\left(\frac{r_m - |x|}{\omega}\right) + \frac{1}{2}\right] \quad (2)$$

Here, x is the vector offset from the image center, $|x|$ the distance from the image center, r_m is the maximum radius of the pattern in the image, and k_m specifies the maximum instantaneous frequency. Furthermore, tanh can be seen as an approximation to a step function, where r_m is the location of the step and ω is the width of the transition. The following parameters were used to generate the test patterns: $k_m = \frac{\pi}{2}$, $r_m = 400$, and $\omega = 40$.

Figures 7 and 8 only use the lower half of the Jähne pattern, due to its symmetry. Arrows were placed on a radial line to demonstrate the effects of varying frequency and constant perceived direction of the background texture. Furthermore, by arranging arrows on circular paths, the impact of changing perceived direction of the background texture and a constant spatial frequency are shown. Figure 7a shows the original image where some arrows seems to be rotated by several degrees. This effect is compensated in Figure 7b.

5 MULTIFIELD FLOW VISUALIZATION

So far, our method was demonstrated only for artificial stimuli. In this section, results of a compensation for an example from scientific visualization are presented. In such a scenario, foreground textures might be glyphs or other small graphical elements that are superimposed over a background texture to provide additional localized information.

We discuss a specific, yet typical example from scientific flow visualization: the simultaneous plot of two 2D vector fields in a single image (Urness et al., 2006). One of the vector fields may be visualized by arrow glyphs that yield a coarse representation. A complementary visualization is chosen for the other vector field and shown as background texture. Here, we use a dense texture-based method in the form of line integral convolution (LIC) (Cabral and Leedom, 1993). This method allows us to visualize fine details of vector fields that might be hard to detect in the coarse grids of glyphs. For more background on texture-based flow visualization, we refer to the survey paper by Laramee et al. (2004).

In such an example use case, the simultaneous orientation contrast between the LIC background and the glyph foreground can result in a tilt illusion. Mis-

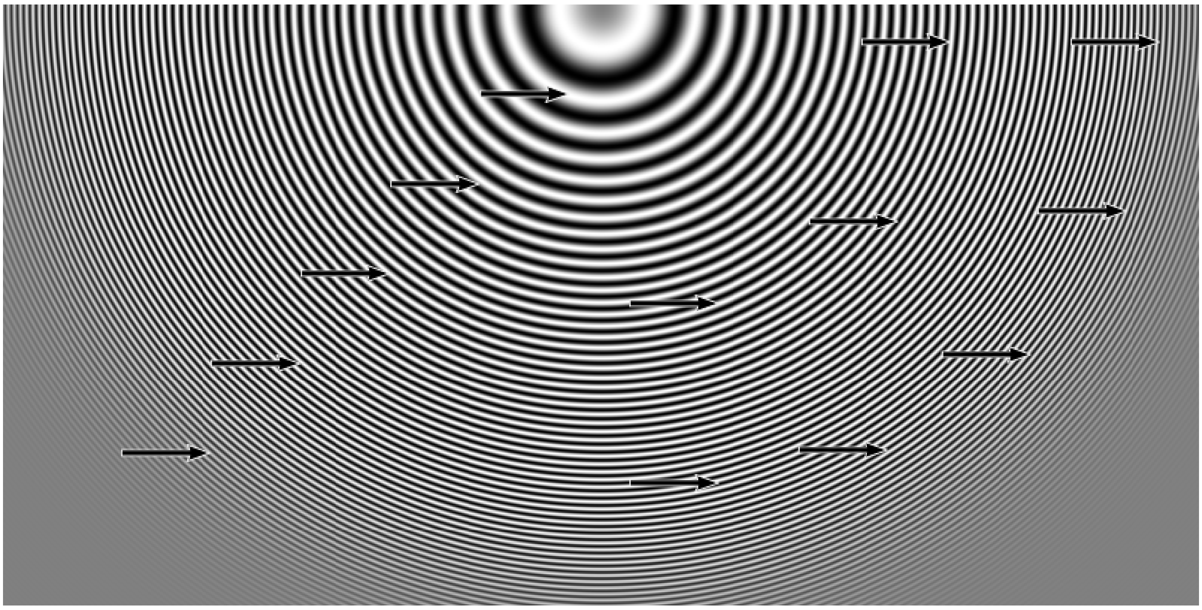

(a) Without compensation

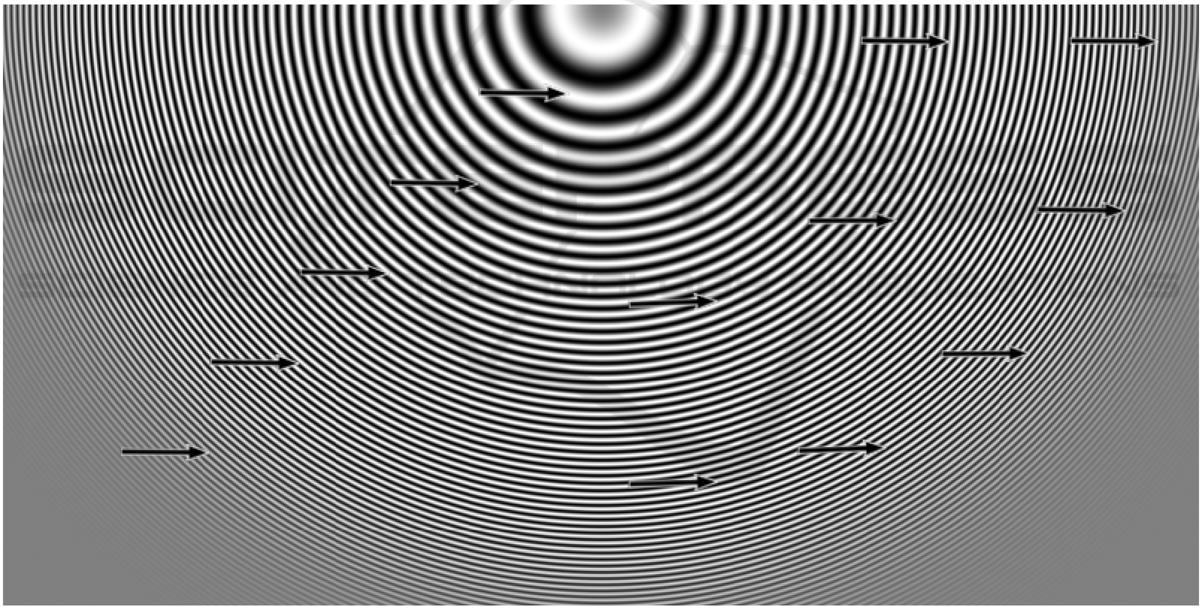

(b) With compensation

Figure 7: Arrows are superimposed on a Jähne test pattern. On the left side, for each arrow position, the frequency is changing and the direction of the background texture is constant. On the right side, arrows are arranged on two circles leading to a constant frequency and a varying direction. In a viewing distance of about 20 cm, some arrows seem to be tilted in (a). This effect is compensated in (b). In (b), eight arrows are rotated clockwise (minimum 0.51°, maximum 0.86°, and average 0.69°) and five arrows are rotated counterclockwise (minimum 0.36°, maximum 2.28°, and average 1.38°).

perceptions in the orientation of superimposed arrows can then lead to false readings of flow direction. Therefore, compensation is crucial for a correct interpretation of the vector fields. Figure 9a shows an example without compensation. Here, an analyst might have selected a region that is of interest and manually placed arrows. For this example, we assume that all glyphs should be perfectly horizontal. Tilt bias from orientation contrast creates the appearance of the lower three arrows going in slightly different directions, while the upper five are not affected. After compensation, all glyphs appear horizontal in Figure 9b. The proposed method works on each arrow individually, i.e., the glyphs are rotated against

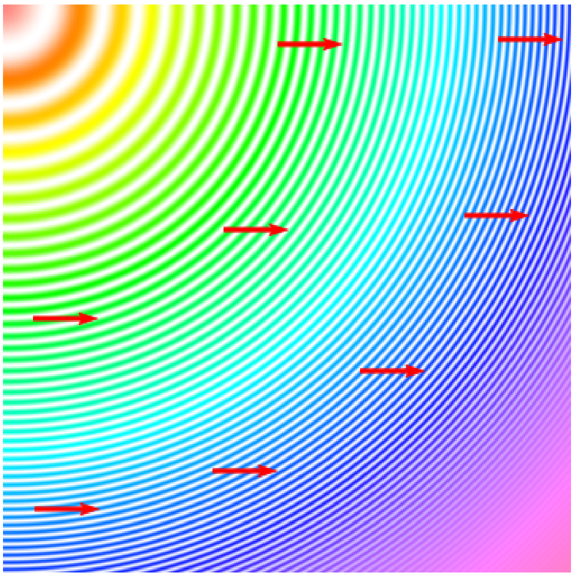

Figure 8: Arrows are superimposed on a Jähne test pattern. They are arranged on two circles, leading to a constant frequency and a varying direction. When texture is rendered with color, the tilt effect is less pronounced than in Figure 7a.

the tilt angle derived at the respective location on the LIC background.

6 DISCUSSION

Our tests with different artificial stimuli show promising results and we were able to demonstrate that our method can be applied in realistic scenarios from flow visualization. However, there are a few topics that require further investigation to improve the compensation and to test its validity.

The first issue concerns the weight functions. Our frequency weight seems to be reliable, since it is based on the results of an experiment that specifically tested the effects of frequency on the tilt bias. This is not the case for the contrast weight. Here, we were only able to use four measurements of an experiment that measured the after effects of tilt illusions in the case of a simultaneous appearance of fore- and background texture. In both cases, it would be beneficial to verify the results of the frequency experiment and to improve the contrast weight function by conducting experiments with a more appropriate sampling of the parameter space.

We based our method on the tilt bias of Schwartz et al. (2009), who used measurements from Westheimer (1990). In this original work, the author conducted experiments using only vertically oriented stimuli, but states on page 1914 that "there is no reason to believe that the findings [...] would not apply to other orientations". However, viewing our test images vertically or horizontally can lead to the perception of varying degrees of the tilt illusion, depending on the observer. This suggests the existence of an additional parameter to the tilt effect and requires further investigation.

(a) Image without compensation

(b) Image with compensation

Figure 9: Arrows superimposed on background LIC textures that depict a vector field. The three arrows at that bottom of (a) are affected by the tilt illusion at a viewing distance of about 20 cm. In the compensated image (b), they appear horizontal. In (b), four arrows are rotated clockwise (0.76°, 2.47°, 0.08°, and 1.71°) and four arrows are rotated counterclockwise (2.31°, 0.96°, 1.42°, and 2.23°).

Another aspect that is not addressed yet is the impact of color on the tilt illusion. This was subject of previous research (Clifford et al., 2003a; Lovegrove and Over, 1973; Clifford et al., 2003b), where measurements were taken with respect to color signals (L, M, and S cone signals derived from RGB images) and luminance. Color contrast can reduce the tilt effect, as shown in Figure 8. Here, the tilt effect is weaker than in Figure 7a. In the best case, Equation 1 might simply be extended by additional weight terms for the influence of color. In the worst case, there could be dependencies between color, contrast, and frequency that would need to be modeled.

The next topic that could be of relevance is to incorporate Gestalt laws into the compensation process. For instance, horizontally aligned arrows on a virtual horizontal line are less influenced by the tilt bias according to our observations of initial tests. The human visual system relies on certain expectations or makes assumptions in the presence of geometric structures. This issue is even more pronounced for large foreground objects that may require nonlinear and spatially dependent deformations for tilt compensation.

A related topic is the estimation of the dominant frequency and direction. As described in Section 3, the maximum response for direction and frequency is currently utilized. However, Figure 5b shows that there might be several distinct local maxima that could be considered for compensation, in particular, for large textures.

7 CONCLUSION

In this paper, we addressed the topic of visual illusion effects; more specifically, the tilt illusion caused by simultaneous orientation contrast. It is a relevant topic within the field of visualization, as it can occur when overlaying textures or even in line renderings.

We have proposed an approach to compensate for the tilt illusion in case of superimposed textures. This is of practical relevance for visualization since superimposed textures are commonly used for multifield and other overlaid visualizations. To perform the compensation, information about directions, frequencies, and contrast are extracted from the input images. Based on the results of prior experiments on the effects of the tilt illusion, we have approximated weight functions for frequency and contrast, which are used to avoid overcompensation. We demonstrate the results of our method for artificial stimuli and a realistic scenario from flow visualization.

In our example cases, the results are promising. However, a misinterpretation of the visualization is only prevented for specific stimuli, render sizes, viewing distances and subjects; all of which we cannot control. While someone looks at the digital version of this paper on a screen, someone else prints it with or without scaling, holds it nearer to the eyes while reading, etc. In short, there are still a number of topics that need to be addressed. One of them is that our efforts resulted in a compensation success that varies between each individual person. More work is needed to explore the effects of simultaneous orientation contrast. Our method might benefit from additional experiments to refine the weight functions, the incorporation of color or Gestalt laws, and, finally, the handling of secondary maxima in the weighting of perceived directions and frequencies.

ACKNOWLEDGEMENTS

We would like to thank the German Research Foundation (DFG) for financial support within project B01 of SFB/Transregio 161.

REFERENCES

Bair, A. and House, D. H. (2007). Grid with a view: optimal texturing for perception of layered surface shape. *IEEE Transactions on Visualization and Computer Graphics*, 13(6):1656–1663.

Bair, A., House, D. H., and Ware, C. (2009). Factors influencing the choice of projection textures for displaying layered surfaces. In *Proceedings of the 6th Symposium on Applied Perception in Graphics and Visualization (APGV)*, pages 101–108.

Becker, R. A., Eick, S. G., and Wilks, A. R. (1995). Visualizing network data. *IEEE Transactions on Visualization and Computer Graphics*, 1(1):16–28.

Cabral, B. and Leedom, L. C. (1993). Imaging vector fields using line integral convolution. In *Proceedings of the SIGGRAPH Annual Conference on Computer Graphics and Interactive Techniques*, pages 263–270.

Carter, R. (2014). *The Brain*. Dorling Kindersley Ltd.

Clifford, C. W., Pearson, J., Forte, J. D., and Spehar, B. (2003a). Colour and luminance selectivity of spatial and temporal interactions in orientation perception. *Vision Research*, 43(27):2885 – 2893.

Clifford, C. W. G., Spehar, B., Solomon, S. G., Martin, P. R., and Qasim, Z. (2003b). Interactions between color and luminance in the perception of orientation. *Journal of Vision*, 3(2).

Durant, S. and Clifford, C. W. G. (2006). Dynamics of the influence of segmentation cues on orientation perception. *Vision Research*, 46(18):2934–2940.

Franceschiello, B., Sarti, A., and Citti, G. (2018). A neuromathematical model for geometrical optical illusions. *Journal of Mathematical Imaging and Vision*, 60(1):94–108.

Frintrop, S., Rome, E., and Christensen, H. I. (2010). Computational visual attention systems and their cognitive foundations: a survey. *ACM Transactions on Applied Perception*, 7(1):6:1–6:39.

Georgeson, M. A. (1973). Spatial frequency selectivity of a visual tilt illusion. *Nature*, 245:43.

Goodenough, D. R., Oltman, P. K., Sigman, E., Rosso, J., and Mertz, H. (1979). Orientation contrast effects in the rod-and-frame test. *Perception & Psychophysics*, 25(5):419–424.

Healey, C. G. and Enns, J. T. (2012). Attention and visual memory in visualization and computer graphics. *IEEE Transactions on Visualization and Computer Graphics*, 18(7):1170–1188.

Jähne, B. (2004). *Practical Handbook on Image Processing for Scientific and Technical Applications, Second Edition*. CRC Press, Inc.

Kirby, R. M., Marmanis, H., and Laidlaw, D. H. (1999). Visualizing multivalued data from 2D incompressible flows using concepts from painting. In *Proceedings of the IEEE Visualization Conference*, pages 333–340.

Laramee, R. S., Hauser, H., Doleisch, H., Vrolijk, B., Post, F. H., and Weiskopf, D. (2004). The state of the art in flow visualization: dense and texture-based techniques. *Computer Graphics Forum*, 23(2):203–222.

Lovegrove, W. and Over, R. (1973). Colour selectivity in orientation masking and aftereffect. *Vision Research*, 13(5):895–901.

Luboschik, M., Radloff, A., and Schumann, H. (2010). A new weaving technique for handling overlapping regions. In *Proceedings of the International Conference on Advanced Visual Interfaces (AVI)*, pages 25–32.

Mittelstädt, S. and Keim, D. A. (2015). Efficient contrast effect compensation with personalized perception models. *Computer Graphics Forum*, 34(3):211–220.

Mittelstädt, S., Stoffel, A., and Keim, D. A. (2014). Methods for compensating contrast effects in information visualization. *Computer Graphics Forum*, 33(3):231–240.

Molotchnikoff, S. and Rouat, J., editors (2012). *Visual Cortex - Current Status and Perspectives*. InTech.

Nothdurft, H. (1991). Texture segmentation and pop-out from orientation contrast. *Vision Research*, 31(6):1073–1078.

Palmer, S. E. (1999). *Vision Science: Photons to Phenomenology*. MIT Press.

Schwartz, O., Sejnowski, T. J., and Dayan, P. (2009). Perceptual organization in the tilt illusion. *Journal of Vision*, 9(4):19–19.

Urness, T., Interrante, V., Longmire, E., Marusic, I., O'Neill, S., and Jones, T. W. (2006). Strategies for the visualization of multiple 2D vector fields. *IEEE Computer Graphics and Applications*, 26(4):74–82.

Ware, C. (2012). *Information Visualization: Perception for Design*. Morgan Kaufmann, third edition.

Wei, H., Ren, Y., and Li, B.-M. (2013). A collaborative decision-making model for orientation detection. *Applied Soft Computing*, 13(1):302–314.

Weiskopf, D. (2004). On the role of color in the perception of motion in animated visualizations. In *Proceedings of the IEEE Visualization 2004 Conference*, pages 305–312.

Westheimer, G. (1990). Simultaneous orientation contrast for lines in the human fovea. *Vision research*, 30(11):1913–1921.

Zhou, L. and Hansen, C. D. (2016). A survey of colormaps in visualization. *IEEE Transactions on Visualization and Computer Graphics*, 22(8):2051–2069.